Biosensors and Bioelectronics 26 (2011) 4656–4660

Contents lists available at ScienceDirect

Biosensors and Bioelectronics

journal homepage: www.elsevier.com/locate/bios

Carbon nanoparticle for highly sensitive and selective fluorescent detection of mercury(II) ion in aqueous solution

Hailong Li[a,b], Junfeng Zhai[a], Jingqi Tian[a,b], Yonglan Luo[a], Xuping Sun[a,*]

[a] State Key Lab of Electroanalytical Chemistry, Changchun Institute of Applied Chemistry, Chinese Academy of Sciences, Changchun 130022, Jilin, China
[b] Graduate School of the Chinese Academy of Sciences, Beijing 100039, China

ARTICLE INFO

Article history:
Received 24 December 2010
Received in revised form 19 March 2011
Accepted 27 March 2011
Available online 2 April 2011

Keywords:
Carbon nanoparticle
Fluorescence
Hg^{2+} detection
T–Hg^{2+}–T

ABSTRACT

In this article, carbon nanoparticles (CNPs) were used as a novel fluorescent sensing platform for highly sensitive and selective Hg^{2+} detection. To the best of our knowledge, this is the first example of CNPs obtained from candle soot used in this type of sensor. The general concept used in this approach is based on that adsorption of the fluorescently labeled single-stranded DNA (ssDNA) probe by CNP via π–π stacking interactions between DNA bases and CNP leads to substantial dye fluorescence quenching; however, in the presence of Hg^{2+}, T–Hg^{2+}–T induced hairpin structure does not adsorb on CNP and thus retains the dye fluorescence. A detection limit as low as 10 nM was achieved. The present CNP-based biosensor for Hg^{2+} detection exhibits remarkable specificity against other possible metal ions. Furthermore, superior selectivity performance was observed when Hg^{2+} detection was carried out in the presence of a large amount of other interference ions. Finally, in order to evaluate its potential practical application, Hg^{2+} detection was conducted with the use of lake water other than pure buffer and it is believed that it holds great promise for real sample analysis upon further development.

1. Introduction

Mercury(II) ion (Hg^{2+}) is a highly toxic heavy metal ion and considered as one of the most dangerous and ubiquitous pollutants (Renzoni et al., 1998). Its contamination comes from a variety of natural sources as well as human activities (Harris et al., 2003), and an annual release was 4400–7500 metric tons estimated by the United Nations Environment Programme (UNEP) (Liu and Lu, 2007). It have been demonstrated that Hg^{2+} can easily pass through skin, respiratory, and gastrointestinal tissues into the human body and damage the central nervous and endocrine systems (Gutknecht, 1981), which raises serious environmental and health concerns. So there is an ever-growing demand to develop effective analytical methods for sensitive and selective detection of Hg^{2+}. Indeed, the past years have witnessed increasing research efforts in this direction and many detection methods have been established (Chen and He, 2004; Chiang et al., 2008; Li et al., 2009, 2010; Guo et al., 2009; Huang et al., 2007; Kim and Bunz, 2006; Liu and Lu, 2007; Miller and Chang, 2007; Wang et al., 2005, 2007, 2008; Wegner et al., 2007; Yoon et al., 2005; Zhang et al., 2008). Traditionally, Hg^{2+} is detected by atomic absorption/emission spectroscopy, Auger-electron spectroscopy, inductively coupled plasma mass spectrometry, or ion selective electrode or polarography (Guo et al., 1996; Wang et al., 2007); however, these methods require sophisticated instrumentation and/or sample preparation, which limits their practical applications. To solve these problems, alternative methods using small-molecule-based fluorescent probe (Chiang et al., 2008; Descalzo et al., 2003; Miller and Chang, 2007; Nolan and Lippard, 2003; Wang et al., 2005; Yoon et al., 2005; Zhang et al., 2008), DNAzymes (Liu and Lu, 2007; Vannela and Adriaens, 2007; Darbha et al., 2008; Li et al., 2009), protein (Chen and He, 2004; Wegner et al., 2007), conjugated polymers (Kim and Bunz, 2006), gold nanoparticles (Huang et al., 2007; Liu et al., 2008; Wang et al., 2008), and semiconductor quantum dots (Guo et al., 2009) have also been developed in the past years. However, each of these methods has its own drawbacks, such as poor selectivity, insufficient resolution in aqueous media, high detection limit, and/or sophisticated synthesis of the probe materials. Although highly selective and sensitive detection of Hg^{2+} has been reported recently (Chiang et al., 2008; Huang et al., 2007; Liu et al., 2008), it still remains a great challenge to develop other new methods for this kind of detection, which will provide more insights for the development.

On the other hand, oligonucleotide (OND) has also been proven to be a versatile tool for the detection of metal ions due to their specific interactions. The conformation of OND can be induced to fold into a hairpin structure by metal ion such as Hg^{2+} through T–Hg^{2+}–T base pairs (Miyake et al., 2006), providing a rationale to design T-rich OND-based sensor for Hg^{2+}. Indeed, Ono et al.

* Corresponding author. Tel.: +86 431 85262065; fax: +86 431 85262065.
E-mail address: sunxp@ciac.jl.cn (X. Sun).

0956-5663/$ – see front matter © 2011 Elsevier B.V. All rights reserved.
doi:10.1016/j.bios.2011.03.026

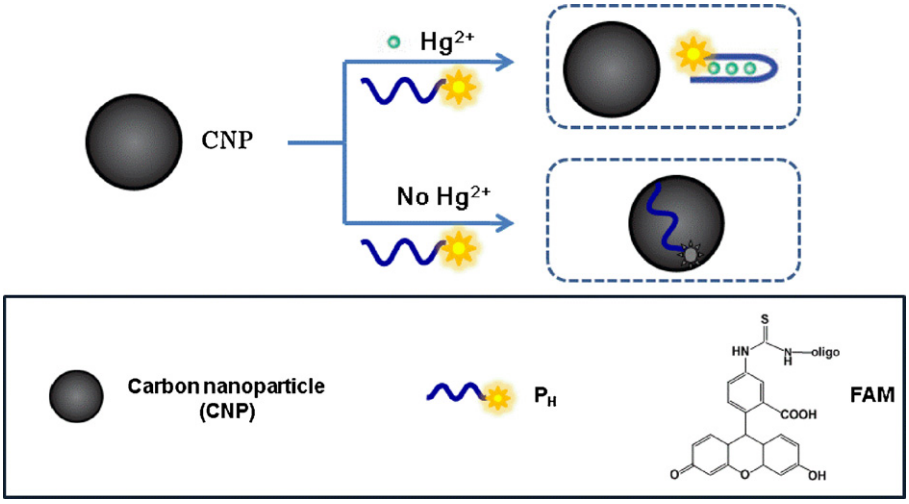

Scheme 1. A schematic (not to scale) illustrating the CNP-based fluorescent Hg^{2+} detection based on conformational change of a Hg^{2+}-specific T-rich OND (P_H). P_H: a FAM-labeled Hg^{2+}-specific OND probe.

have developed a fluorescent Hg^{2+} sensor using a T-rich OND, dual-labeled with a fluorescent dye and a quencher at each terminus (Ono and Togashi, 2004). In the presence of Hg^{2+}, the chelating of Hg^{2+} into mismatched T–T base pair induces the formation of a hairpin structure, which brings both termini close to each other, resulting in significant quenching of the dye fluorescence. More recently, nanostructures including single-walled carbon nanotubes (SWCNTs) (Zhang et al., 2010), graphene oxide (GO) (He et al., 2010) and nano-C_{60} (Li et al., 2011a) have been used to quench the dye of a single-labeled fluorescent OND probe and as an effective fluorescent sensing platform for sensitive and selective Hg^{2+} detection. However, SWCNT, graphite (used for GO preparation) and C_{60} (used for nano-C_{60} preparation) must be purchased from some sources. On the other hand, SWCNT treatment and GO preparation by Hummers method (Hummers and Offeman, 1958) is time-consuming and labor-intensive. Accordingly, new sensing platform which can overcome all these shortcomings is highly desirable. In this article, we demonstrate the first use of carbon nanoparticles (CNPs), relatively inexpensive carbon materials obtained from candle soot, as a fluorescent sensing platform for highly sensitive and selective detection of Hg^{2+}, expecting to extend the use of this emerging kind of nanocarbon (Sheila and Gary, 2010). The general concept used in this approach is based on that adsorption of the fluorescently labeled single-stranded DNA (ssDNA) probe by CNP via π–π stacking interactions between DNA bases and CNP (Li et al., 2011b; Varghese et al., 2009) leads to substantial fluorescence quenching; however, in the presence of Hg^{2+}, T–Hg^{2+}–T induced hairpin structure does not adsorb on CNP and thus retains the dye fluorescence. Scheme 1 presents a schematic to illustrate the CNP-based fluorescent Hg^{2+} detection.

2. Experimental

2.1. Chemicals and instruments

The chemically synthesized oligonucleotide was purchased from Shanghai Sangon Biotechnology Co. Ltd. (Shanghai, China). DNA concentration was estimated by measuring the absorbance at 260 nm. All the other chemicals were purchased from *Aladin* Ltd. (Shanghai, China) and used as received without further purification. Metal ion solutions were prepared from corresponding chloride salt. The water used throughout all experiments was purified through a Millipore system.

Scanning electron microscopy (SEM) measurements were made on a XL30 ESEM FEG scanning electron microscope. Transmission electron microscopy (TEM) measurements were made on a HITACHI H-8100 EM (Hitachi, Tokyo, Japan). Fluorescent emission spectra were recorded on a RF-5301PC spectrofluorometer (Shimadzu, Japan). Zeta potential measurements were performed on a Nano-ZS Zetasizer ZEN3600 (Malvern Instruments Ltd., U.K.).

Oligonucleotide sequence is listed as follows:

P_H (FAM dye-labeled ssDNA probe for Hg^{2+}):
5′-TTC TTT CTT CCC CTT GTT TGT T-FAM-3′

2.2. Carbon nanoparticles preparation

CNPs were prepared as follows: Too small CNPs (below 10 nm) produce strong photoluminescence emission interfering with detection (Sheila and Gary, 2010) and too large CNPs tend to sink during the measurements, so CNPs with suitable size should be selected. In brief, 3-mg candle soot obtained using well-established method (Liu et al., 2007) was suspended in 12-mL water–ethanol mixture (1:1) with the help of ultrasonication for 30 min. After that, the black solution was centrifuged at 3000 rpm for 2 min to separate out large carbon soot particle and the supernatant was collected. Subsequently, the collected supernatant was subjected to centrifugation at 6000 rpm for 2 min. Too small CNPs still suspended in the liquid and were discarded, the black precipitate was collected and redispersed in 12-mL water–ethanol mixture (1:1) for further characterization and sensing application. We repeat the separation and collected the desired CNPs, both of water and ethanol can be removed by lyophilization. According to the mass of the precipitation after drying, the concentration of previously prepared suspension is about 0.15 mg/mL.

For scanning electron microscopy (SEM) characterization, 20 μL of the suspension was placed on an indium tin oxide (ITO) glass slide and air-dried at room temperature. SEM measurements were made on a XL30 ESEM FEG scanning electron microscope at an accelerating voltage of 20 kV. The sample for transmission electron microscopy (TEM) measurements was prepared by placing a dilution of colloidal solution on a carbon-coated copper grid and drying at room temperature. TEM measurements were made on a HITACHI H-8100 EM (Hitachi, Tokyo, Japan) with an accelerating voltage of 200 kV.

2.3. Fluorescence spectroscopic studies

For fluorescence measurements, excitation was at 480 nm and the emission was monitored at 518 nm. The volume of each sample is 400 μL in 20 mM Tris-HCl buffer containing 100 mM NaCl and 5 mM KCl (pH: 7.4). The volume of CNPs is 20 μL used for each fluorescence quenching. All the experiments were carried out at room temperature (about 25 °C) if not specified.

3. Results and discussion

Too small CNPs (below 10 nm) produce strong photoluminescence emission interfering with detection (Sheila and Gary, 2010) and too large CNPs tend to sink, therefore, suitable CNPs should be selected. Lots of work has been focused on the preparation of smaller fluorescent carbon nanodots (Sheila and Gary, 2010), however, such carbon nanoparticles do not meet the requirement for the use as a fluorescent sensing platform because their own fluorescence will produce interference. Jia et al. have reported the preparation of carbon sphere with bigger size from glucose, which needs high temperature and special equipments (Jia et al., 2009). Recently, we have prepared carbon nanosphere from graphite, involving the use of chlorosulphonic acid and microwave (Li et al., 2011c). Here, in our present study, only a simple separation process was involved to collect CNPs with desired size from candle soot, a relatively inexpensive carbon material obtained by lighting a candle (Liu et al., 2007). Fig. S1A shows the low magnification SEM image of the resulting products, indicating that they consist of a large amount of nanoparticles. The high magnification image shown in Fig. S1B further reveals that they are nearly spherical with unsmoothed surface and in the range of 25–40 nm, which is also evidenced by the corresponding TEM images, as shown in Fig. S1C and D. It is also important to mention that the obtained CNPs have a zeta potential of −7.19 mV and are well-dispersed in water–ethanol mixture; however, it is impossible to obtain reliable overall information about the CNPs existing in solution by using SEM and TEM techniques because the evaporation of the solvent during the sample preparation may lead to secondary aggregations of the CNPs on the substrate used (Sun et al., 2003).We firstly compared the fluorescence intensity of the probe-CNP complex in the absence and presence of Hg^{2+}, respectively. Fig. 1A shows the fluorescence emission spectra of FAM-labeled ssDNA, P_H, under different conditions. In the absence of CNPs, P_H exhibits strong fluorescence emission due to the presence of the fluorescein-based dye (curve a). However, the presence of CNPs results in about 84% quenching of the fluorescence emission (curve c), indicating that the CNP can adsorb ssDNA and quench the fluorescent dye very effectively. The adsorption of ssDNA can be supported by the experimental fact that the fluorescence intensity of supernatant of probe-CNP complex is slightly influenced after removing CNPs from the solution by centrifugation (Fig. S2). Only a little of P_H existed in the aqueous solution because most of them were adsorbed on CNPs and the slight fluorescence intensity enhancement can be attributed to more or less release of ssDNA from CNPs during centrifugation. Like GO and SWCNTs, CNP is also a π-rich structure, the fluorescence quenching of FAM-labeled P_H may be induced by electron transfer between CNPs and FAM (He et al., 2010; Li et al., 2011a,b,c; Zhang et al., 2010). In the presence of 4 μM Hg^{2+}, the fluorescence intensity is 4.6-fold higher than that without Hg^{2+} (curve d). It should be pointed out that the fluorescence of free P_H was slightly influenced by Hg^{2+} in the absence of CNPs (curve b). The ability of CNPs to support ssDNA was also investigated (Fig. S3). From the fluorescence quenching efficiency when probe-CNP complex was treated with ultrasonication for different time, it can be concluded that the condition of ultrasonication produced only a little release of probe from CNPs, indicating the excellent stability of nanoprobe. For sensitivity study, different concentrations of Hg^{2+} in the range of 0–10 μM were investigated. Fig. 1B shows the fluorescence intensity of P_H-CNP in the presence of different Hg^{2+} concentrations in Tris–HCl buffer solution. It is clearly seen that the fluorescence intensity of the mixture increases with the increase of Hg^{2+} concentration. Fig. 1B inset is the fluorescence intensity plotted against the logarithm of Hg^{2+} concentration. Even at concentration as low as 50 nM, the fluorescence intensity is distinct from that without Hg^{2+}. On the basis of the plot in the inset of Fig. 1B, the fluorescence intensity reaches a platform at the concentration of 10 μM, implying the occurrence of saturation. The detection limit is estimated to be 10 nM (three times the standard deviation of the blank solution), which is much lower than that on SWCNT (Zhang et al., 2010) and GO (He et al., 2010). We speculate the reason for the much high sensitivity of CNP compared to the SWCNT and GO could be due to its spherical morphology and unsmoothed surface, but the exact reason is not completely understood at present time. All the above observations indicate that the present sensing system has high sensitivity and holds a promising potential for practical application. It is also important to mention that although CNPs tend to sink in the mixing solution of water and ethanol, they can be well-dispersed by shaking and kept stable during our measurements.

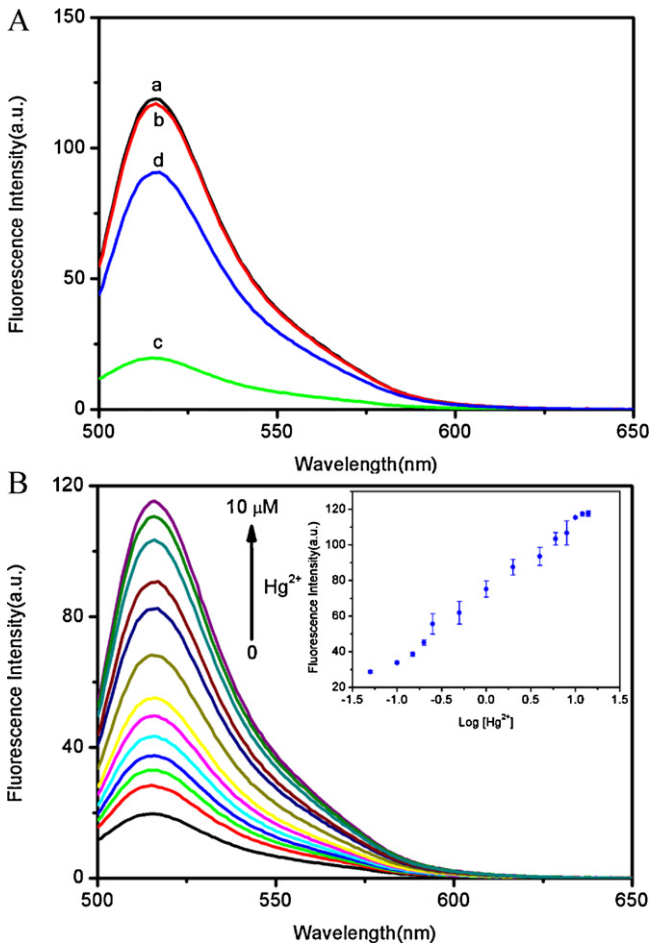

Fig. 1. (A) The fluorescence spectra of: (a) P_H, (b) $P_H + Hg^{2+}$, (c) P_H + CNPs, and (d) P_H + CNPs + Hg^{2+}, respectively. (B) Fluorescence spectra of P_H + CNPs in the presence of different Hg^{2+} concentrations (from bottom to top: 0, 0.05, 0.1, 0.15, 0.2, 0.25, 0.5, 1.0, 2.0, 4.0, 6.0, 8.0, and 10.0 μM). The inset is the fluorescence intensity plotted against the logarithm of Hg^{2+} concentration. Excitation was at 480 nm and the emission intensity was monitored at 518 nm. All measurements were done in Tris–HCl buffer (pH 7.4) ([P_H]: 100 nM; [Hg^{2+}]: 4 μM).

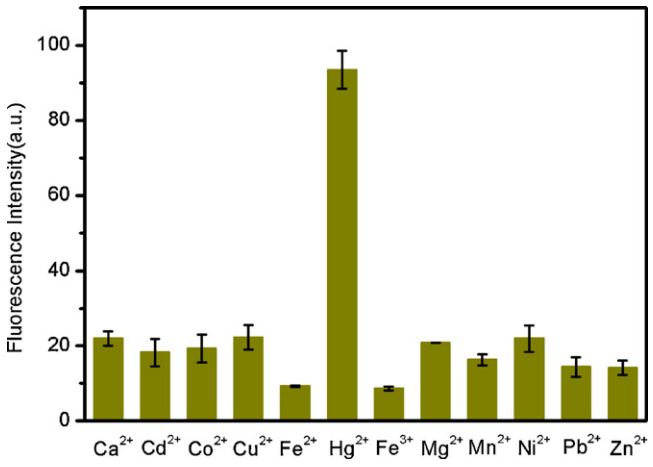

Fig. 2. Fluorescence intensity histograms of P_H + CNPs in the presence of different metal ions ([Hg^{2+}] = 4 μM; [other metal ion] = 50 μM) with error bar (standard deviation from the mean, n = 3). Excitation was at 480 nm and the emission intensity was monitored at 518 nm. All measurements were done in Tris–HCl buffer (pH 7.4) ([P_H]: 100 nM).

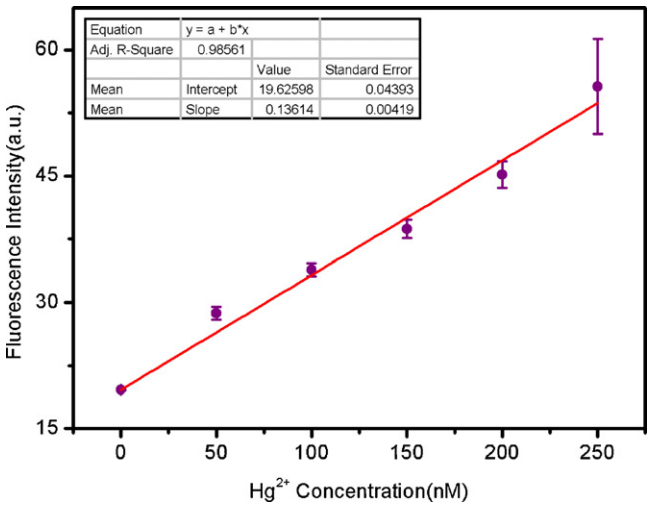

Fig. 4. Linear relationship of the fluorescence intensity of P_H + CNPs in the presence of Hg^{2+}, covering the range from 0 to 250 nM. Excitation was at 480 nm and the emission intensity was monitored at 518 nm ([P_H]: 100 nM).

Next, we evaluated the specificity of the present system for Hg^{2+} detection. To do this, a variety of environmentally relevant metal ions including Ca^{2+}, Cd^{2+}, Co^{2+}, Cu^{2+}, Fe^{2+}, Fe^{3+}, Hg^{2+}, Mg^{2+}, Mn^{2+}, Ni^{2+}, Pb^{2+}, and Zn^{2+} were examined. We firstly investigated whether these metals alone can quench FAM-labeled ssDNA probe, P_H. It is found that these metal ions do not cause much impact on the fluorescence intensity of P_H in the absence of CNPs except Fe^{2+}, Fe^{3+}, and Pb^{2+} (Fig. S4). In spite of fluorescence quenching to FAM induced by Fe^{2+}, Fe^{3+}, or Pb^{2+}, the specificity is increased in contrast for the suggested CNP-based nanoprobe. Fig. 2 shows the difference in fluorescence intensity of solutions containing Hg^{2+} (4 μM) or other metal ions (50 μM) in the presence of CNPs. It can be clearly seen that the relative large amount of the other metal ions has small influence on the fluorescence of the system, indicating the sensing system described herein exhibits high specificity for Hg^{2+} against other metal ions. Furthermore, the selectivity of this nanoprobe in the presence of any possible interference ions is evaluated. As demonstrated in Fig. 3, obviously, the present method can still detect Hg^{2+} in the presence of all any possible interference ions. The fluorescence intensity with 4 μM Hg^{2+} (curve b) is 2.5-fold higher than that without Hg^{2+} (curve a). The above results indicated that this CNP-based fluorescent sensor for Hg^{2+} detection possesses outstanding specificity and selectivity against other interference metal ions.

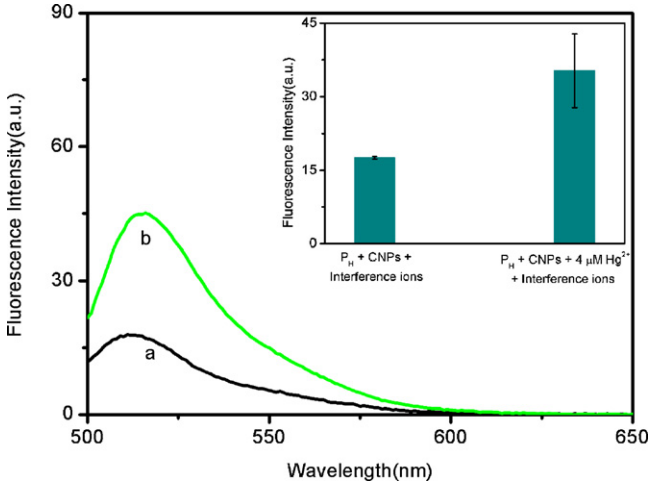

Fig. 3. Fluorescence spectra of (a) P_H + CNPs and (b) P_H + CNPs + Hg^{2+} in the presence of any possible metal ions, including Ca^{2+}, Cd^{2+}, Co^{2+}, Cu^{2+}, Fe^{2+}, Fe^{3+}, Mg^{2+}, Mn^{2+}, Ni^{2+}, Pb^{2+}, and Zn^{2+}. The inset is the corresponding histograms with error bar (standard deviation from the mean, n = 3). ([Hg^{2+}] = 4 μM; [other metal ion] = 10 μM). Excitation was at 480 nm and the emission intensity was monitored at 518 nm. All measurements were done in Tris–HCl buffer (pH 7.4) ([P_H]: 100 nM).

In addition to investigating the Hg^{2+} sensor in an artificial system using pure buffer, the performance of the present method for real sample analysis was also evaluated. Lake water samples were obtained from the South Lake of Changchun, Jilin province, China. In order to avoid the interference from oil and other organic and biological impurities existing in environmental water, samples were filtered through a column packed with anionic exchange resin to remove them (Wang et al., 2008). ICP-MS was used to verify that the lake water samples did not contain Hg^{2+}. Thereafter, water samples spiked with different concentrations of Hg^{2+} were determined using the suggested method (assay mixture contains 100 nM of P_H and 20-μL CNPs). Hg^{2+} concentration can be calculated from the fluorescence intensity according to the linear relationship in the range from 0 to 250 nM Hg^{2+}, as indicated in Fig. 4. The calibration curve of the whole range from 0 to 10 μM and the linear regression at higher concentration of Hg^{2+} (0.5–10 μM) is demonstrated in Fig. S5. Table 1 lists the concentration determination of Hg^{2+} using both the present method and ICP-MS. Based on the comparison, the results obtained by our suggested approach are in good agreement with those from ICP-MS. It can detect as low as 30 nM Hg^{2+}, which satisfies the sensitivity requirement for Hg^{2+} detection in drinking water (30 nM) defined by WHO (Zhang et al., 2010). The results clearly suggest that our method could be used for the quantification of Hg^{2+} in practical samples.

Table 1
Sensing of Hg^{2+} in lake water samples using the present method and ICP-MS.

Samples	Spiked (nM)	The present method[a] mean ± SD (nM)	ICP-MS mean ± SD (nM)
1	0	0	0 ± 0.02
2	30	26.23 ± 6.90	30.05 ± 0.45
3	60	61.86 ± 2.74	60.23 ± 0.55
4	120	123.79 ± 4.72	121.85 ± 0.64

[a] Mean of three determinations; SD: standard deviation.

4. Conclusions

In summary, we demonstrate the first use of CNPs as an effective sensing platform for fluorescent Hg^{2+} detection with high sensitivity and specificity. The selectivity performance is outstanding when Hg^{2+} detection was carried out in the presence of all any possible interference ions. A detection limit as low as 10 nM is obtained. Such CNPs are obviously easier to produce and thus the CNP-based Hg^{2+} detection platform is practically more important than that based on SWCNT and GO (Zhang et al., 2010; He et al., 2010). It is believed that this sensing platform will find great application in real environmental analysis.

Acknowledgement

This work was supported by National Basic Research Program of China (No. 2011CB935800).

Appendix A. Supplementary data

Supplementary data associated with this article can be found, in the online version, at doi:10.1016/j.bios.2011.03.026.

References

Chen, P., He, C., 2004. J. Am. Chem. Soc. 126, 728–729.
Chiang, C.K., Huang, C.C., Liu, C.W., Chang, H.T., 2008. Anal. Chem. 80, 3716–3721.
Darbha, G.K., Singh, A.K., Rai, U.S., Yu, E., Yu, H., Ray, R.C., 2008. J. Am. Chem. Soc. 130, 8038–8043.
Descalzo, A.B., Martínez-Máñez, R., Radeglia, R., Rurack, K., Soto, J., 2003. J. Am. Chem. Soc. 125, 3418–3419.
Gutknecht, J.J., 1981. J. Membr. Biol. 61, 61–66.
Guo, T., Baasner, J., Gradl, M., Kistner, A., 1996. Anal. Chim. Acta 320, 171–176.
Guo, W., Yuan, J., Wang, E., 2009. Chem. Commun., 3395–3397.
Harris, H.H., Pickering, I.J., George, G.N., 2003. Science 301, 1203- 1203.
He, S., Song, B., Li, D., Zhu, C., Qi, W., Wen, Y., Wang, L., Song, S., Fang, H., Fan, C., 2010. Adv. Funct. Mater. 20, 453–459.
Huang, C.C., Yang, Z.S., Lee, K.H., Chang, H.T., 2007. Angew. Chem. Int. Ed. 46, 6824–6828.
Hummers, W.S., Offeman, R.E., 1958. J. Am. Chem. Soc. 80, 1339- 1339.
Jia, G., Yang, M., Song, Y., You, H., Zhang, H., 2009. Cryst. Growth Des. 9, 301–307.
Kim, B., Bunz, U.H.F., 2006. J. Am. Chem. Soc. 128, 2818–2819.
Li, D., Song, S., Fang, C., 2010. Acc. Chem. Res. 43, 631–641.
Li, H., Zhai, J., Sun, X., 2011a. Nanoscale, doi:10.1039/c1nr10052a.
Li, H., Zhang, Y., Wang, L., Tian, J., Sun, X., 2011b. Chem. Commun. 47, 961–963.
Li, H., Zhang, Y., Wu, T., Liu, S., Wang, L., Sun, X., 2011c. J. Mater. Chem. 21, 4663–4668.
Liu, C.W., Hsieh, Y.T., Huang, C.C., Lin, Z.H., Chang, H.T., 2008. Chem. Commun., 2242–2244.
Liu, H., Ye, T., Mao, C., 2007. Angew. Chem. Int. Ed. 46, 6473–6475.
Liu, J., Lu, Y., 2007. Angew. Chem. Int. Ed. 46, 7587–7590.
Li, T., Li, B., Wang, E., Dong, S., 2009. Chem. Commun., 3551–3553.
Miller, E.M., Chang, C.J., 2007. Curr. Opin. Chem. Biol. 11, 620–625.
Miyake, Y., Togashi, H., Tashiro, M., Yamaguchi, H., Oda, S., Kudo, M., Tanaka, Y., Kondo, Y., Sawa, R., Fujimoto, T., Machinami, T., Ono, A., 2006. J. Am. Chem. Soc. 128, 2172–2173.
Nolan, E.M., Lippard, S.J., 2003. J. Am. Chem. Soc. 125, 14270–14271.
Ono, A., Togashi, H., 2004. Angew. Chem. Int. Ed. 43, 4300–4302.
Renzoni, A., Zino, F., Franchi, E., 1998. Environ. Res. 77, 68–72.
Sheila, N.B., Gary, A.B., 2010. Angew. Chem. Int. 49, 6726–6744.
Sun, X., Jiang, X., Dong, S., Wang, E., 2003. Macromol. Rapid Commun. 24, 1024–1028.
Vannela, R., Adriaens, P., 2007. Environ. Eng. Sci. 24, 73–84.
Varghese, N., Mogera, U., Govindaraj, A., Das, A., Maiti, P.K., Sood, A.K., Rao, C.N.R., 2009. Chem. Phys. Chem. 10, 206–210.
Wang, H., Kang, B., Chancellor, T.F., Lele, T.P., Tseng, Y., Ren, F., 2007. Appl. Phys. Lett. 91, 042114–042116.
Wang, H., Wang, Y., Jin, J., Yang, R., 2008. Anal. Chem. 80, 9021–9028.
Wang, L., Wong, W.K., Wu, L., Li, Z., 2005. Chem. Lett. 34, 934–935.
Wegner, S.V., Okesli, A., Chen, P., He, C., 2007. J. Am. Chem. Soc. 129, 3474–3475.
Yoon, S., Albers, A.E., Wong, A.P., Chang, C.J., 2005. J. Am. Chem. Soc. 127, 16030–16031.
Zhang, L., Li, T., Li, B., Li, J., Wang, E., 2010. Chem. Commun., 1476–1478.
Zhang, X., Xiao, Y., Qian, X., 2008. Angew. Chem. Int. Ed. 47, 8025–8029.